Carbohydrate Polymers 339 (2024) 122247

Contents lists available at ScienceDirect

Carbohydrate Polymers

journal homepage: www.elsevier.com/locate/carbpol

High-amylose starch-based gel as green adhesive for plywood: Adhesive property, water-resistance, and flame-retardancy

Yaoxing Chen [a,1], Yongjing Rao [a,1], Peng Liu [a,*], Linlin Wu [a], Guojie Zhang [a], Jianguo Zhang [a,*], Fengwei Xie [b,*]

[a] School of Chemistry and Chemical Engineering, Guangzhou University, Guangzhou Higher Education Mega Center, Guangzhou, Guangdong 510006, China
[b] Department of Chemical Engineering, University of Bath, Bath BA2 7AY, United Kingdom

ARTICLE INFO

Keywords:
Starch-based adhesives
Biopolymer-based gels
High-amylose starch
Water-resistance
Wood flame retardancy

ABSTRACT

The escalating demand for environmentally sustainable and cost-effective adhesives in the wood processing and manufacturing sector has prompted exploration into innovative solutions. This study introduces a novel gel adhesive composed of chemically unmodified high-amylose starch (G70, with 68 % amylose content) with a minimal proportion of urea-formaldehyde (UF) (UF/starch = 1:10, *w*/w). This G70/UF gel demonstrates remarkable adhesive capabilities for wooden boards under both dry conditions (with a shear stress of 4.13 ± 0.12 MPa) and wet conditions (with a shear strength of 0.93 ± 0.07 MPa after 2 h of water soaking). The study unveils that the elevated amylose content in the starch, coupled with a meticulously controlled isothermal process during bonding, is crucial for these enhancements. Specifically, the robust cohesion of amylose chains expedites phase separation between starch and UF, while the isothermal process facilitates the migration and enrichment of UF molecules at the gel-board and gel-air interfaces. Lacking these mechanisms, conventional amylopectin-rich starch/UF gels (27 % amylose content) show minimal improvement. Moreover, the G70/UF gel showcases exceptional fire retardancy. In all, the G70/UF gel presents a promising alternative for plywood production, reducing reliance on unhealthy UF resin while offering satisfactory bonding resistance in diverse conditions and superior flame retardancy.

1. Introduction

In the wood processing and manufacturing industry, a diverse range of adhesives are currently employed, such as polyvinyl acetate (PVAc), epoxy, polyurethane, and condensation resins, and among them, formaldehyde-based condensation resins represent the largest volume (Dunky, 2003). These condensation resins are created through the reaction of formaldehyde with various chemicals such as urea, melamine, phenol, resorcinol, or their combinations. The widely used urea-formaldehyde (UF) resin, known for its affordability, strong bonding, and water resistance, finds extensive application in the production of wood-based composite materials, such as plywood, particleboards, and medium-density fiberboards (MDF) (Dorieh et al., 2022).

Nevertheless, UF resins have drawbacks and environmental concerns, with one being the gradual release of formaldehyde gas, contributing to indoor air pollution, potential respiratory irritation, and other health issues. Consequently, there is a growing demand for bio-based 'green' adhesives to replace petrochemical adhesive components, such as soybean protein, natural tannin, and starch (Watcharakitti et al., 2022). Among these alternatives, starch, as a renewable, readily available, and cost-effective biopolymer, emerges as a promising candidate for the development of bio-based wood adhesives (Gadhave et al., 2017).

Starch has a rich history as an adhesive globally. In China, historical evidence indicates the use of sticky rice as building mortar in the construction of The Great Wall (Qi & Can, 2013). By the ninth century, starch was employed for sizing papers (Onusseit, 1992). In Egypt, it served as a binder for crafting papyrus (Radley, 1976), while in France, decorative wall hangings affixed with flour pastes emerged before 1630 (Radley, 1976).

The adhesive ability of native starch gel primarily stems from its abundant hydroxyl groups, enabling it to adhere strongly to materials rich in hydroxyl groups, like paper. However, native starch gel proves unsuitable as a wood adhesive due to its weak bonding strength and

* Corresponding authors.
E-mail addresses: liu_peng@gzhu.edu.cn (P. Liu), jianguo.zhang@gzhu.edu.cn (J. Zhang), dx335@bath.ac.uk (F. Xie).
[1] Both are the first authors.

https://doi.org/10.1016/j.carbpol.2024.122247
Received 8 February 2024; Received in revised form 16 April 2024; Accepted 7 May 2024
Available online 8 May 2024

inadequate water resistance (Din et al., 2020). Hence, modifications are necessary to enhance the functionality of starch-based adhesives (Maulana et al., 2022), and modified starches include acid-hydrolyzed starch, oxidized starch, vinyl acetate grafted starch (Zia ud et al., 2018), and crosslinked starch with a silane coupling agent (Chen et al., 2017). Despite providing commendable adhesive properties for starch gels, these chemical modifications entail a complex production process (Zia-ud-Din et al., 2017).

Another effective approach to enhance the performance of starch-based wood adhesives involves combining starch with other components, such as PVOH (Vineeth & Gadhave, 2024), UF resin (Oktay et al., 2021), and tannins (Oktay et al., 2022). Notably, composite adhesives using UF resin and starch have garnered significant attention from researchers. Jarusombuti et al. (Jarusombuti et al., 2012) developed medium-density fiberboards (MDF) bonded with native cassava starch and UF and found that boards with 3 % UF and 10 % starch met the Japanese Industrial Standard A-5908. However, they did not elaborate on the board properties in the wet state.

Oxidized starch is a common choice for composite adhesives, given its ability to enhance bonding and water resistance (Din et al., 2020). Sulaiman et al. (Sulaiman et al., 2018) crafted a single-layer particleboard with UF resin and epichlorohydrin-modified starch and reported that the panels met the minimum required strength according to Japanese Industrial Standards (JIS). Wang et al. (Wang et al., 2017) incorporated oxidized starch into UF resin in the final stage and noted an improvement in resin bond strength. Although composite adhesives exhibit commendable bonding properties in both dry and wet states, the complex and environmentally impactful production process of oxidized starch underscores the urgent need for eco-friendly starch-based adhesives in wood-based materials.

The adhesive abilities come in two ways: the adhesive force on the interface and the cohesive force within the matrix. Amylopectin, which has high hydroxyl density, offers superior adhesive force. Related to this, in ancient China, waxy rice was often used to prepare glue. Conversely, amylose exhibits high cohesion, thereby enhancing the gel matrix. In recent years, heightened attentions has been paid to high-amylose starch-based adhesives because of the robust cohesive force resulting from inter-amylose chain interactions (Diyana et al., 2021; Obadi et al., 2023). Our group has devised a facile method to disorganize high-amylose starch granules (Y. Li et al., 2020; Xi et al., 2024). Building on this, we prepared high-amylose starch-based gels and compared their adhesive properties with those of normal starch-based gels (Liu et al., 2023). The results revealed that the robust cohesion among amylose chains could diminish water absorption but had minimal impact on bonding properties since adhesive force mainly relies on the hydrogen bonds formed at the interface between gel and wooden board. Besides, excessive cohesion, as seen in the G70 starch gel, which contains 68 % amylose content, led to peeling off from a wood surface after storage.

Considering the previously observed weak adhesive force of starch-based gels on wooden boards, this study introduces UF resin into starch-based gels and investigates its impact on gel characteristics. Our hypothesis was that certain phase separation between amylose and UF could lead to the enrichment of UF on the interface between wooden board and gel, which can maximize adhesive effects and water resistance. Our results demonstrate that even minor additions of UF resin prove instrumental in significantly enhancing the bonding performance and water resistance of high-amylose starch-based gels. Consequently, plywood prepared with this composite adhesive exhibits commendable mechanical properties in both dry and wet states, along with an excellent flame-retardant feature.

2. Materials and methods

2.1. Materials

Normal corn starch (NCS, 27 % amylose content) was purchased from Dezhou Dacheng Food Co., Ltd. (China). Two high-amylose corn starches (HACS), labeled as G50 (55 % amylose content) and G70 (68 % amylose content), were supplied by Jiangsu Sanshu Bio-technology Co., Ltd. (China). Anhydrous calcium chloride and silicone oil (DC 200) were bought from Sigma-Aldrich (Shanghai) Trading Co., Ltd. and were both analytically pure. Urea-formaldehyde resin (UF, powder, containing 1 % ammonium chloride) was offered by Guangdong Ruicai Technology Co., Ltd. Polyvinyl acetate (PVAc) was purchased from Anhui Dizhi Chemical Technology Co., Ltd.

2.2. Preparation of starch-based gel

The preparation of starch-based gel can be seen in Fig. 1. First, 12.5 g of anhydrous $CaCl_2$ was added into 25 mL of distilled water to prepare a $CaCl_2$ solution with a mass concentration of 33 %. Subsequently, 10 g of starch was added to the $CaCl_2$ solution to form a starch slurry. The slurry was then placed into a three-necked flask and stirred at 75 °C for 30 min, yielding a starch solution. Simultaneously, 1 g of UF resin was blended with 1 mL of water to create a resin slurry. This resin slurry was introduced into the starch solution, and the mixture was stirred at 75 °C for another 30 min, ultimately resulting in a starch-based gel.

2.3. Characterization of the adhesive property of starch-based gels

For bonded samples, pieces of *Paulownia fortunei* wooden boards measuring 38 mm × 25 mm × 1 mm were selected. The starch-based gel, maintained in a liquid state at 75 °C, was evenly applied (about 0.05 g) onto the surface of two wooden boards (10 mm × 25 mm). The coated area was compressed tightly, and the samples were immediately placed in an oven, isothermal set at 75 °C for 4 h. After that, the samples were transferred to a closed environment at room temperature with 50 % relative humidity (RH) for 24 h to achieve moisture equilibrium.

For samples bonded by UF resin, UF powder was mixed with water at a ratio of 5:3 (*w*/w). The resulting slurry (about 0.05 g) was coated on wooden boards and subjected to the same isothermal conditions. In the case of PVAc, it was directly coated (about 0.05 g) onto wooden boards and subjected to the same isothermal parameters.

The formaldehyde content in G70/UF gel was detected according to the Chinese National Standard (GB/T 23993–2009). Specifically, 2.0 g of G70/UF gel was added into 250 mL of deionized water, and the mixture was heated and distilled. 200 mL of the distillate was collected and diluted to 250 mL. Then, 10 mL of the solution was collected and mixed with 5 mL of acetylacetone solution (0.25 %, *v*/v), and the mixture was heated in a boiled water bath for 3 min. After that, the sample was detected by UV–vis spectrometry (U-2910, Hitachi Japan Ltd) at 415 nm. The content was calculated based on a standard curve established beforehand.

To evaluate the adhesive property of the starch-based gel, shear strength tests were conducted according to the Chinese national standard (GB/T 33333–2016). Following moisture equilibration, shear strength was measured on wooden boards in both dry (no contact with water) and wet states (soaking in water at 25 °C for 2 h).

A texture analyzer (TPA, SMS/TA.XT Plus, Stable Micro Systems LTD, United Kingdom) with a 50 kg load cell was used for shear strength testing. The two ends of the bonded wooden boards were secured by the fixtures of the texture analyzer, and the extension rate was maintained at 0.5 mm/s. For each sample, at least five tests (based on five specimens) were performed.

2.4. Chemical and structural analysis of starch-based gel

2.4.1. Fourier transform infrared (FTIR) spectroscopy

To investigate the functional groups and chemical characteristics of starch-based adhesives, Fourier-transform infrared spectroscopy (Thermo Scientific iN10, USA) was employed. The adhesives were freeze-dried into powder and mixed with KBr to form pellets, which

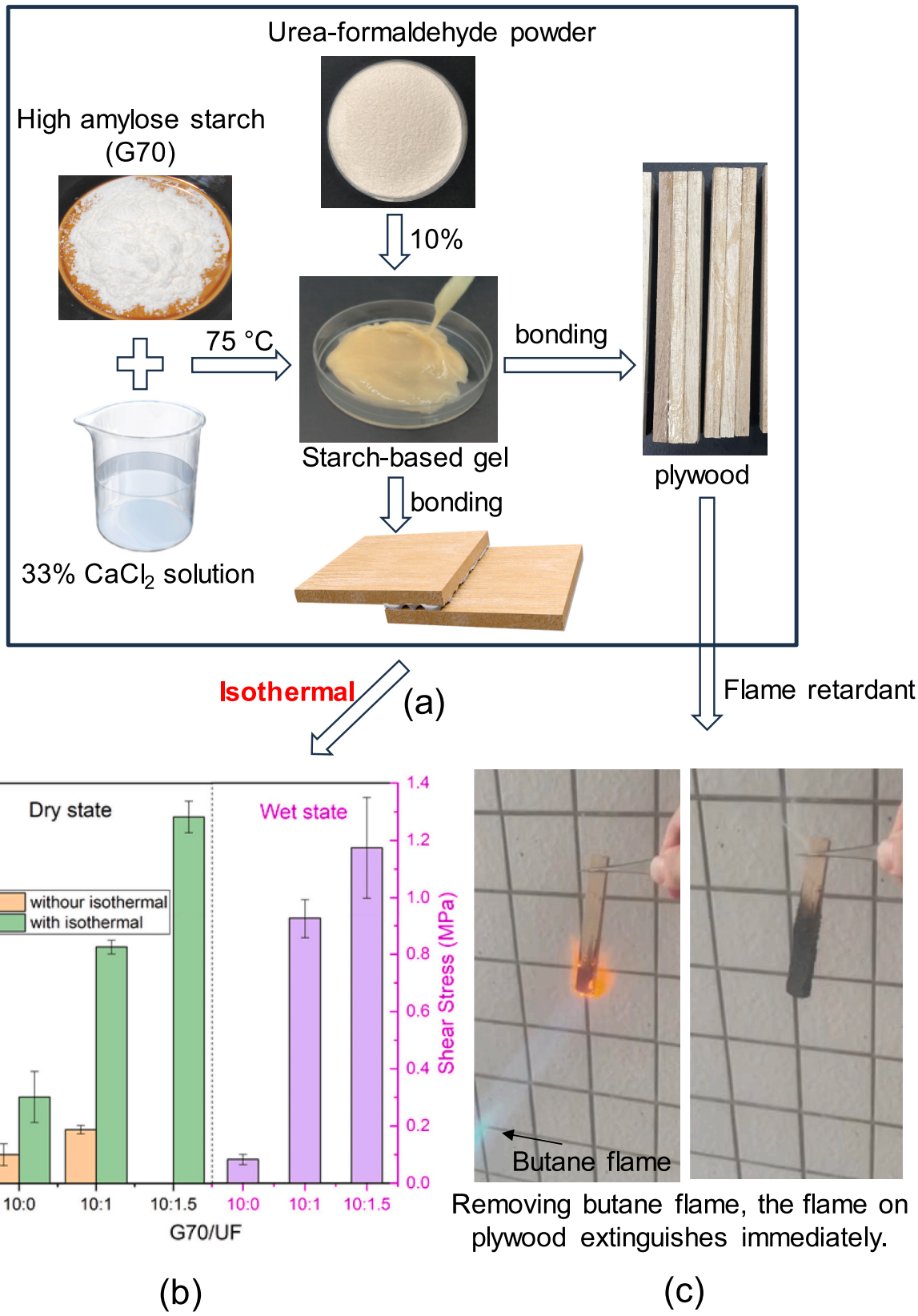

Fig. 1. Preparation of starch-based gel (a); its adhesive property under dry and wet conditions (b); and its flame retardancy (c).

were scanned in the range of 400 to 4000 cm^{-1} for 16 cycles.

2.4.2. Nitrogen content analysis tests

For nitrogen content analysis, starch-based gels were kept in a liquid state at 75 °C and poured into a cylindrical mold (25 mm in diameter, 18 cm in height). The mold underwent isothermal conditions in an oven (at temperatures of 60 °C, 70 °C, 75 °C, 80 °C, and 90 °C; for durations of 1 h, 2 h, and 4 h). Following this, the cylinder was placed in a closed

environment at room temperature with 50 % RH for 24 h to achieve moisture equilibrium. Subsequently, the samples (about 3 mg) were extracted from both the surface and the center of the cylinder. Nitrogen content on these different parts was measured using an elemental analyzer (Vario EL Cube, Elementar Analysensysteme GmbH, Germany), and the ratio of nitrogen content on the surface to that in the center was calculated. For each sample, at least three tests were performed.

2.4.3. X-ray photoelectron spectroscopy (XPS) analysis

Test samples were extracted from the surface and the interior (10 mm from the surface) of NCS/UF and G70/UF gels. These samples underwent composition analysis using a Thermo Scientific K-Alpha X-ray photoelectron spectrometer. Analysis was conducted under vacuum (pressure $< 10^{-8}$ mbar) with a pass energy of 150 eV for survey scans. Spectra for C1s, O1s, and N1s were obtained for meticulous examination. Calibration of all peaks was performed using the C1s peak binding energy at 284.8 eV for adventitious carbon. Data refinement was carried out using Thermo Advantage software.

2.5. Characterization of the surface hydrophilicity and rheological properties of starch-based gel

2.5.1. Water contact angle testing

The water contact angle values of starch-based gel surfaces were measured using a contact angle meter (JY-PHB, Chengde Jinhe Instrument Manufacturing Co., Ltd., China). Using a cylindrical-shaped gel as the sample, the water contact angle was determined by placing a 10 μL drop of deionized water on its surface.

2.5.2. Rheological analysis

For the examination of the dynamic viscoelastic behavior of starch-based gels, an MCR 92 rheometer (Anton Paar GmbH, Graz, Australia) equipped with a 50 mm parallel plate and a temperature control system was used. The distance between the two plates was set at 1.0 mm, the strain at 1 %, the frequency at 1 Hz, and the temperature ramp to be from 30 to 100 °C. To maintain sample moisture content, silicone oil (DC 200) was applied around the edge of the measuring cell.

2.6. Molecular simulation for the phase separation

Utilizing coarse-grained molecular simulation technology, we investigated phase separation and UF molecule enrichment within the amylose matrix during an isothermal process. The simulations of polymer mixture solutions were performed within a 50 σ × 50 σ × 127 σ simulation box, covering the x, y, and z directions, respectively. In the solution, two types of polymer were modeled as bead-spring linear chains following the Kremer-Grest model (Kremer & Grest, 1990). The longer polymer (P_l) comprises 100 coarse-grained (CG) beads, representing amylose chains, while the shorter polymer (P_s) consists of 10 CG beads, representing UF molecules. The solvent molecule (S) is modeled as a single bead identical to the polymer monomer. All polymer and solvent beads have mass (m) and interact via a shifted Lennard-Jones (LJ) 12–6 pairwise potential, as shown by Eq. (1):

$$U_{LJ}(r) = 4\varepsilon\left[\left(\frac{\sigma}{r}\right)^{12} - \left(\frac{\sigma}{r}\right)^{6} - \left(\frac{\sigma}{r_c}\right)^{12} + \left(\frac{\sigma}{r_c}\right)^{6}\right] \quad (1)$$

where r, σ, and ε are the distance between the centers of two beads, the size of beads and the strength of the interaction between them, respectively. A cutoff distance of $r_c = 3.0\,\sigma$ was applied to all non-bonded pairs. The detailed interaction parameters are listed in Table S1. Bonding interactions between connected polymer beads are governed by the finitely extensible nonlinear elastic (FENE) potential, as shown by Eq. (2):

$$U_B(r) = -\frac{1}{2}KR_0^2 ln\left[1 - \left(\frac{r}{R_0}\right)^2\right] \quad (2)$$

where r is the bond length and $R_0 = 1.5\,\sigma$ and $K = 30\,\varepsilon/\sigma^2$.

The simulation system comprises 1000 long polymer chains, 1000 short chains, and 100,000 solvent molecules, resulting in an initial polymer volume fraction of about 50 %. To confine the position of the polymer film, a solid surface (six-layered FCC lattice) was introduced at the bottom of the simulation box, with the parameters of the interactions between the solid surface and other molecular beads (polymer and solvent) listed in Table 1.

All the simulations were carried out with LAMMPS (Plimpton, 1995) During equilibration, the temperature T was maintained at 1.0 ε/k_B by weakly coupling all solution beads to a Langevin thermostat with a damping constant 0.1 τ^{-1}, where the time unit (τ) is defined as $\tau = \sqrt{m\sigma^2/\varepsilon}$. The equations of motion were integrated using a Velocity-Verlet algorithm with a time step $\delta_t = 0.005\,\tau$. Evaporation was triggered by removing gas molecules from the top of the simulation box at a fixed speed of 1 molecule per 100 timesteps. Throughout evaporation, the Langevin thermostat was removed and the Berendsen thermostat with a coupling time of 0.5 was used to control the solid surface temperature ($T = 1.0\,\varepsilon/k_B$). Periodic boundary conditions are applied across all three spatial dimensions.

2.7. Preparation of plywood and three-point bending testing

Three-layer plywood was prepared using G70/UF gel, UF resin, and PVAc, respectively. Specifically, *Paulownia fortunei* wooden boards measuring 80 mm × 10 mm × 4 mm were selected as bonded samples. The starch-based gel, in a liquid state at 75 °C, and the UF resin slurry (prepared by mixing UF powder with water at a 5:3 w/w ratio) were applied to the wooden board surfaces at a dosage of 50 g/m^2. Following this, the plywood underwent pressing under 1 MPa pressure for 5 min and was then placed in a 75 °C oven for 4 h. The samples were stored at room temperature (25 °C, 50 % RH) for 24 h before testing.

After moisture equilibration, the flexural strength and flexural strain of the plywood were determined using a texture meter (SMS/TA.XT Plus) under dry and wet conditions (after immersion in cold water at 25 °C for 2 h), respectively. All tests were performed at room temperature with a constant crosshead speed of 5.0 mm/min under displacement control. Each sample underwent at least five tests, based on five specimens.

2.8. Detection of the limiting oxygen index (LOI) of plywood

Limiting oxygen index (LOI) is the minimum concentration of oxygen in an oxygen/nitrogen gas stream mixture to maintain combustion, which was used to assess the ignition and ease of extinction of a sample. LOI was performed according to the ISO 4589-2:1996 standard using an HC-2-type instrument (China). Plywood bonded with PVAc, G70/UF gel, and UF resin, with a dimension of 80 mm × 10 mm × 4 mm, was used in all tests.

Table 1
Nonbonded interaction parameters for different interaction pairs.

Pairs	ε	σ
Sol-Sol	1.0	1.0
P_{St}-P_{St}	0.8	1.0
P_{UF}-P_{UF}	1.0	1.0
P_{St}-Sol	0.8	1.0
P_{UF}-Sol	1.1	1.0
P_{St}-P_{UF}	0.9	1.0
Surface-Surface	10.0	1.0
Other-Surface	0.9	1.0

2.9. Statistical analysis

Each measurement was systematically duplicated or, when dictated by the test conditions of the samples, triplicated. Data were represented as mean ± standard deviation. Statistical analysis was carried out using SPSS 20.0 software, with significant differences determined through Duncan's multiple range test and deemed acceptable at a significance level of $p < 0.05$.

3. Results and discussion

3.1. Adhesive property and water resistance of starch/UF adhesives

As depicted in Fig. 1(a), starch/UF gel, a viscous homogeneous fluid at 75 °C, can be effortlessly prepared by mixing starch/$CaCl_2$ gel with UF powder. This gel is adept at bonding wooden boards and facilitating plywood preparation.

Fig. 1(b) shows that, in the dry state without the isothermal process, G70 gel exhibited an original shear stress of only 0.50 ± 0.19 MPa, while G70/UF gel displayed a shear stress of 0.94 ± 0.07 MPa. After the isothermal process, the shear stress of G70/UF gel significantly increased to 4.13 ± 0.12 MPa, four times higher than without isothermal treatment. This surpasses the shear stress of commonly used wood glue, PVAc (1.78 ± 0.44 MPa), but falls short of UF resin, where the adhesive force is so potent that fractures occur on the wooden board rather than in the bonding area. Besides, A higher proportion of UF resin led to higher shear stress.

In a wet state (soaked in water for 2 h) without isothermal treatment, neither G70 gel nor G70/UF gel demonstrated adhesive ability, with the bonded boards easily peelable. Hence, their shear stress could not be detected and was not shown in Fig. 1(b). After isothermal processing, the shear stress of G70 gel was only 0.083 ± 0.017 MPa. In contrast, G70/UF gel, aided by UF resin and isothermal treatment, achieved a shear stress of 0.93 ± 0.07 MPa, marking an over 10-fold increase. This value is higher than the Chinese National Standard 9648–2015 (0.7 MPa). Moreover, an increase in UF molecules within the gel boosted shear stress in the wet state. However, extending the immersion time to 24 h caused the adhesive wooden board to peel off. Put simply, G70/UF gel (10:1) exhibited water resistance capable of withstanding short water exposure, but prolonged contact resulted in deterioration.

In summary, UF resin (starch-to-UF resin ratio of 10:1, *w*/w) and the isothermal process were pivotal factors contributing to the substantial enhancement in adhesive ability and water resistance of G70/UF gel. Besides, a higher proportion of UF resin led to higher shear stress. The typical strain-stress curves for Fig. 1(b) can be seen in Fig. S1(a) and (b).

Besides, G70/UF gel exhibited flame-retardancy, as illustrated in Fig. 1(c). When utilized in plywood preparation, it imparted flame retardancy to plywood. Using a butane flame to ignite the plywood, the flame extinguished immediately upon removing the butane flame. In essence, plywood bonded by G70/UF gel acted as a fire deterrent, preventing the spread of flames. The complete video can be seen in Video Clips S1 and S2.

The formaldehyde content in G70/UF gel (starch-to-UF resin ratio of 10:1, w/w) was 0.414 ± 0.005 g/kg, meeting the requirement of the Chinese National Standard (GB 18583–2008, lower than 1.0 g/kg for water-based adhesives).

3.2. Factors for the improvement in adhesive property and water resistance

Fig. 2 delineates the crucial factors impacting the adhesive property of starch/UF gels after isothermal treatment, encompassing amylose content in starch, $CaCl_2$ concentration used for starch gel preparation, isothermal temperature and time, and storage duration. In our previous study (Liu et al., 2023), using starch gels (without UF resin) to bond wooden boards yielded shear stresses of about 0.4 MPa for NCS gel and 0.5–0.6 MPa for G50 and G70 gel. The influence of amylose content on gels' adhesive ability was found to be insignificant. However, starch gels lacked water resistance, causing bonded wooden boards to peel off upon water exposure. With the addition of UF resin and the isothermal process, shear stresses increased (Fig. 2(a)), measuring 0.54 ± 0.03 MPa for NCS/UF gel, 1.39 ± 0.16 MPa for G50/UF gel, and 4.13 ± 0.12 MPa for G70/UF gel in the dry state. Higher amylose content led to a greater increase. Moreover, in the wet state, boards bonded by starch/UF gels would not peel off after 2 h of water soaking, and the shear stress was detectable, showing improved water resistance. However, G50/UF and NCS/UF gels showed weaker performance, with only G70/UF gel reaching almost 1.0 MPa. Therefore, amylose content emerges as another critical factor influencing the enhanced adhesive ability and water resistance of starch/UF gels. The typical strain-stress curves for Fig. 2(a) can be seen in Fig. S1(c) and (d).

Fig. 2(b) and Fig. 2(c) illustrate the influence of isothermal parameters on the adhesive ability of G70/UF gels. Holding at 60 °C for 4 h resulted in a shear stress of 3.46 ± 0.40 MPa in the dry state. With high isothermal temperatures, shear stress peaked at 75 °C, followed by a slight decrease. In the wet state, a substantial improvement in shear stress occurred from 60 °C to 75 °C, indicating enhanced water resistance. However, a sharp decline from 75 °C to 90 °C suggests that higher isothermal temperatures compromised the water resistance of the gel. Fig. 2(c) reveals that with a shorter isothermal time, shear stress was low in both dry and wet states. Longer isothermal times significantly increased shear stress in both conditions. The typical strain-stress curves for Fig. 2(b) and Fig. 2(c) can be seen in Fig. S1 (e), (f), (g) and (h).

In Fig. 2(d), the influence of $CaCl_2$ solution concentration on the shear stress of G70/UF gels in dry and wet states differed. In the dry state, stress increased with rising $CaCl_2$ concentration, leading to improved adhesive ability. However, in a wet state, excessive $CaCl_2$ reduced shear stress, and the sensitivity of shear stress to $CaCl_2$ concentration was evident, with a 5-fold decrease when the concentration varied from 33 % to 35 %. The typical strain-stress curves for Fig. 2(d) can be seen in Fig. S1(i) and (j).

Fig. 2(e) highlights the stability of the adhesive property of G70/UF gel after a long storage. Shear stress showed no significant variations during a 15-day storage period. In contrast, in our previous study (Liu et al., 2023), wooden boards bonded by G70 gel (without UF resin) gradually became unstuck and peeled off due to high cohesion among amylose chains. The addition of UF resin in this study successfully mitigated this drawback, ensuring the stability of the adhesive property of G70/UF gel. The typical strain-stress curves for Fig. 2(e) can be seen in Fig. S1(k) and (l).

3.3. Mechanism for the improvement of adhesive property and water resistance

3.3.1. FTIR results

To elucidate the presence of chemical crosslinks between starch chains and UF molecules, the FTIR spectra of UF gel were examined (Fig. 3(a)). Characteristic peaks at 1650 cm^{-1} and 1550 cm^{-1} correspond to the C═O and —NH_2 groups of primary amide, while the peak at 1028 cm^{-1} is attributed to CN or NCN stretching of methylene linkages (NCH_2N) (Chiang et al., 2016).

In the case of G70 gel and NCS gel, the characteristic peak at 1640 cm^{-1} can be identified as the water adsorbed in the amorphous region of the starches. The band at 1153 cm^{-1} and 1087 cm^{-1} can be attributed to C—O stretching and C—O—H bending modes, respectively (Kizil et al., 2002). For G70/UF gel and NCS/UF gel, their spectra closely resemble those of the starch gels. The absence of UF gel's characteristic peaks may be attributed to the low amount of UF resin in the gel (1:10, UF/starch, *w*/w). Moreover, no new peaks can be observed in the G70/UF gel spectra, indicating that starch and UF resin are merely physically mixed in the gel. Similar findings were reported by others (Chiang et al., 2016), where particleboards were prepared with UF resin and sago fibers by hot

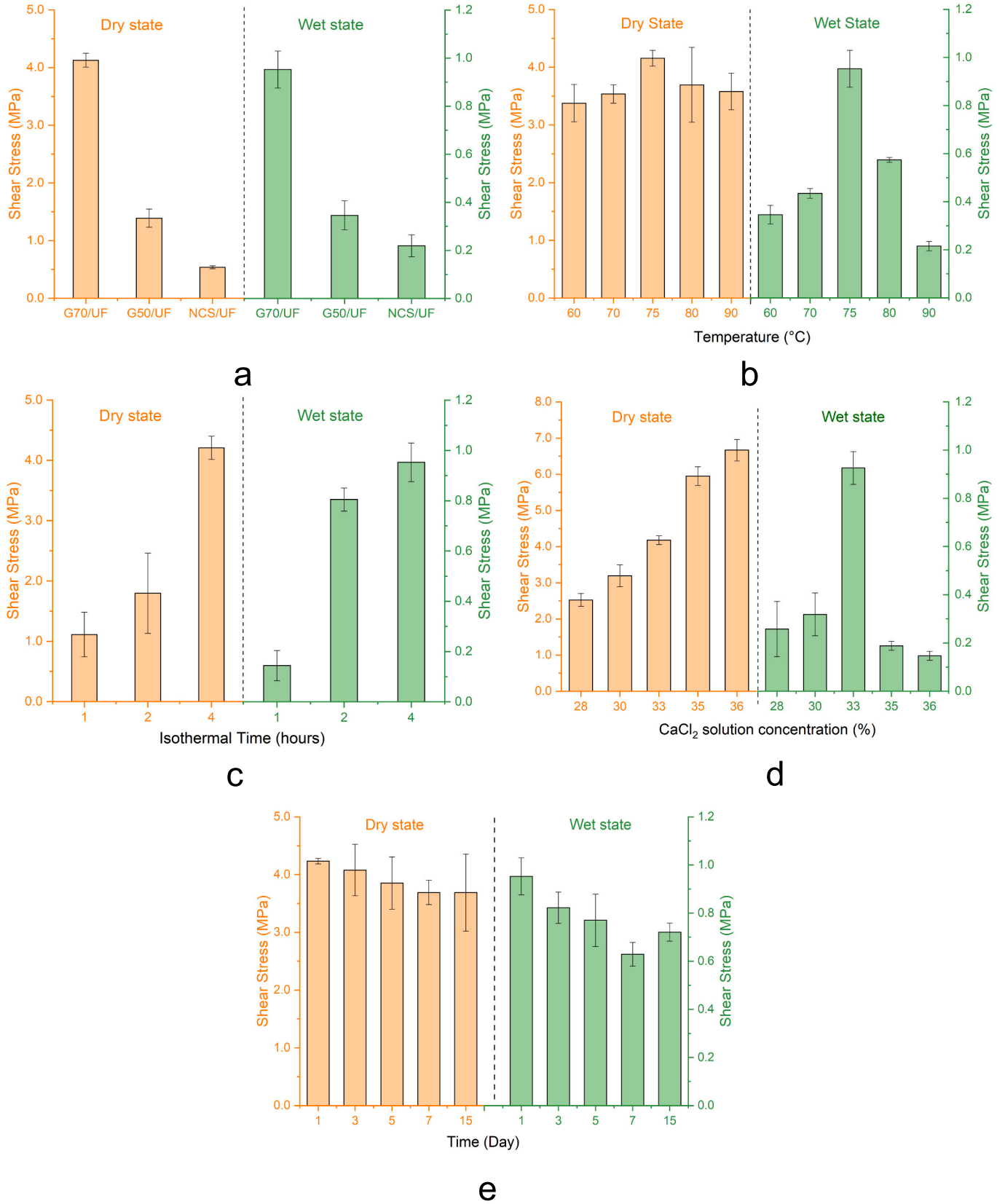

Fig. 2. Factors influencing the shear stress of wooden board adhesive by starch/UF gels. (a) starch/UF gels with different amylose contents; (b) G70/UF gels under different isothermal temperatures; (c) G70/UF gels under different isothermal durations; (d) G70/UF gels with different $CaCl_2$ concentrations; (e) G70/UF gels stored in room condition for different days. Fixed conditions were 33 wt% $CaCl_2$ concentration, isothermal at 75 °C for 4 h, and storage at room condition for 1 days.

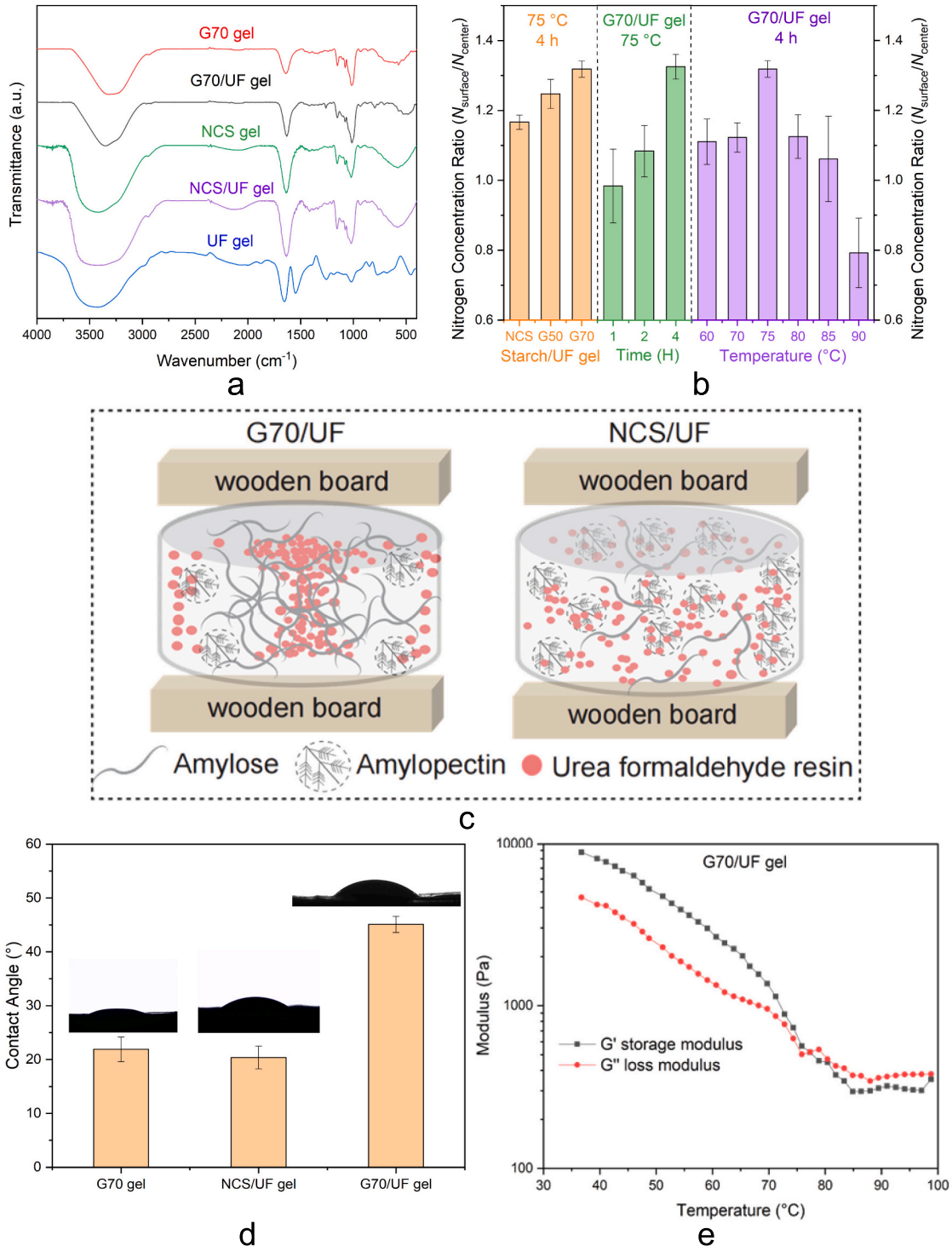

Fig. 3. Mechanism for the enhanced adhesion performance of G70/UF gel. (a) FTIR spectra of the gels; (b) Ratio of nitrogen concentrations on the gel surface versus on the gel interior; (c) Schematic diagram of the phase separation between starch chains and UF molecules when gels were used to bond wooden boards; (d) contact angle results of gels; (e) Dynamic viscoelastic properties of G70/UF gel.

press, revealing no chemical bonds between functional groups of sago starch and UF resin.

3.3.2. *Phase separation between amylose and UF molecules*

Without a chemical reaction, amylose content mainly affects the dispersibility and segregation of UF molecules in the gel. UF resin exhibits robust adhesive force and water resistance after curing (Li et al., 2007). When a small amount of UF resin is introduced into a starch gel (1:10, UF/starch, w/w), it is crucial for the resin to separate from starch chains and come together for effective curing. This process ensures that even minimal additions of UF resin can enhance the adhesive property of the starch-based gel.

However, achieving phase separation in NCS/UF gel proves challenging. In a mixed polymer system, low affinity between polymers is necessary to promote phase separation—referred to as thermodynamic incompatibility, or one polymer's low affinity for the solvent is essential

(Piculell et al., 1995). In the NCS/UF mixed system, the weak thermodynamic incompatibility between starch chains and UF molecules arises because the C═O and —NH_2 groups of UF molecules can form hydrogen bonds with water and starch (Jovanović et al., 2019). Besides, both UF molecules and amylopectin chains, predominantly in NCS gel, exhibit a strong affinity for water (Liu et al., 2023). The acylamino groups on UF molecules can form hydrogen bonds with water molecules. And amylopectin has hydroxyl groups in high density (Long & Christie, 2005), which offer them a strong hydration ability (Fu et al., 2014). No literature reports a significant improvement in adhesive properties and water resistance with the simple mixture of UF resin with normal starch (Maulana et al., 2022).

In contrast, when amylose constitutes the majority in the starch gel (HACS gel), the dynamics change. Amylose, with its long spiral chain conformation, tends to entangle with each other to form double helices through self-association (Arp et al., 2020). This results in low water affinity, making them prone to aggregation and precipitation (Obadi et al., 2023). Starch pastes or foods with high amylose content exhibit rapid chain reassociation or retrogradation (H. Li et al., 2019), showcasing the robust cohesion and aggregation of amylose chains (Liu et al., 2023). Previous studies have reported phase separation in starch paste or amylose/biopolymer mixed systems (BeMiller, 2011), such as glucose (Baba et al., 2021), xanthan (Mandala et al., 2004) and κ-type carrageenan (Tester & Sommerville, 2003). Therefore, based on the self-association of amylose chains, the phase separation of UF molecules in HACS-based gel is facilitated, and higher amylose content in starch makes UF molecule aggregation more achievable.

3.3.3. Curing sites of UF molecules

Besides the segregation, the positioning of UF molecule curing sites within the gel is crucial. If the cured UF resin is buried within the gel, its potent adhesive property remains untapped. Therefore, the curing resin must cure at the gel's surface—specifically at the interfaces between the gel and wood and the gel and air—to effectively enhance the adhesive property and water resistance of G70/UF gel.

To verify this hypothesis, starch/UF gels are shaped into cylinders. After isothermal treatments under different temperatures and durations, nitrogen concentrations on the gel's surface and at its center were measured using an elemental analyzer (Table S1). Subsequently, the nitrogen concentration ratios ($N_{surface}$ vs N_{center}) were calculated (Fig. 3 (b)). Since only UF molecules contain nitrogen, their distribution is reflected by the ratios of nitrogen concentrations at different locations in the gel. Besides, XPS was used to determine nitrogen contents on the surface and at the center of NCS/UF gel and G70/UF gel (Fig. S1).

From Fig. 3(b), the nitrogen concentration ratios for NCS/UF, G50/UF, and G70/UF gels were all higher than 1, indicating the enrichment of UF molecules on the gel's surface. This enrichment can be attributed to the migration of water during the isothermal process, where water migration drove UF molecules to enrich at the interface. Formers have observed that, even for an aqueous solution containing glucose and starch, when drying, the peeling film on the surface was rich in glucose and the remained bottom layer was rich in starch (Baba et al., 2021). This means that as a high molecular weight polymer, the migration ratio of starch can be smaller than those of water and samples with low molecular weight. Therefore, with the addition of UF molecules, shear stresses increased for all starch-based gels (Fig. 2(a)). Moreover, the nitrogen ratio increased with higher amylose content in the gel, demonstrating that amylose accelerated phase separation between starch chains and UF molecules. This facilitated greater UF molecules curing at the interface, promoting the adhesive property of G70/UF gel. Besides, the results of XPS (Fig. S1) further confirm a higher percentage of N1s on the surface of G70/UF gel than in the center.

The structural diagram of starch/UF gels in Fig. 3(c) illustrates that, for G70/UF gel with amylose chains forming the matrix, UF resin cured at the interfaces between the board and gel and between air and gel, offering robust adhesion and water resistance. Besides, since there was only a thin gel layer between wooden boards (about 40–100 μm), UF resin could effectively bond with both the upper and lower wooden boards, ensuring robust cohesion. This prevented slipping or peeling off during the separation of wooden boards. Conversely, in NCS/UF gel, where the matrix was formed by amylopectin and phase separation was less significant, UF molecules would form aggregations within the amylopectin matrix, resulting in a weaker enhancement in the adhesive property.

If the analysis above is accurate, it suggests that the proposed phase segregation could result in G70/UF gel being more hydrophobic than NCS/UF gel. This deduction is supported by Fig. 3(d), where the contact angle rose from 20.4 ± 2.1° for NCS/UF gel to 45.1 ± 1.5° for G70/UF gel.

3.3.4. Influence of isothermal conditions and Ca^{2+} concentrations

Fig. 3(b) illustrates the changes in nitrogen ratios for different isothermal durations and temperatures, which correlate with the variations observed in shear stress depicted in Fig. 2(b) and Fig. 2(c). Specifically, prolonged isothermal durations and elevated temperatures led to increased nitrogen ratios. The anticipated relationship suggests that longer durations allowed for the migration of water and UF molecules, with higher temperatures expediting this process. However, the decline in the ratio beyond 75 °C requires clarification. Specifically, the sol-gel transition temperature for G70/UF gel, as determined by dynamic viscoelastic analysis, (Fig. 3(e)) was 75 °C. Below this temperature, the cohesion of amylose chains was strengthened, facilitating phase separation between them and UF molecules. Conversely, above 75 °C, the increased kinetic energy of amylose chains impeded the migration and aggregation of UF molecules. Consequently, the shear stress and water resistance of the gel reduced at temperatures exceeding 75 °C.

Regarding $CaCl_2$ concentration, there exists a critical threshold concentration of 31 % to thoroughly disorganize G70 starch granules (Y. Li et al., 2020). Below this concentration, amylose remains in aggregated forms rather than forming chains in solution, resulting in a gel matrix primarily composed of amylopectin, akin to that of NCS/UF gel. Consequently, the shear stress exhibited by G70/UF gel with a low Ca^{2+} concentration in a wet state closely resembles that of NCS/UF gel. Furthermore, Ca^{2+} ions have the capability to enhance intermolecular forces between starch chains by coordinating with hydroxyl groups present in starch (Liu et al., 2023). Specifically, Ca^{2+} ions interact with starch via the C6 hydroxyl group of glucosides (Liu et al., 2020), and each Ca^{2+} cation can form connections with multiple hydroxyl groups (Koshevoy et al., 2019), effectively serving as a crosslinker and bolstering the intermolecular force among starch chains. In the case of amylose, which adopts a long spiral chain conformation, coordination primarily occurs between distinct molecular chains, resulting in intermolecular crosslinking. Consequently, besides inducing structural disorganization for amylose aggregates, the introduction of Ca^{2+} ions can not only enhance the cohesion of the amylose matrix but also facilitates phase separation, significantly impacting shear stress. However, it is important to note that $CaCl_2$ is hygroscopic, and excessive remaining $CaCl_2$ promotes water absorption, compromising water resistance. Consequently, higher $CaCl_2$ concentrations in the gel can lead to decreased shear stress in the wet state.

All in all, we have examined the influence of amylose content, isothermal temperature and duration, and $CaCl_2$ concentration on the adhesive properties of starch/UF gels. Among these factors, amylose content emerges as the most significant. Without phase separation, the introduction of UF resin proves ineffective. This explains why UF resin was blended with oxidized starch to bolster adhesive performance in previous studies (Wang et al., 2017). Additionally, the isothermal parameters play a crucial role, as UF molecules can only enrich and cure under suitable conditions.

3.4. Verification of phase transition by molecular simulation

Coarse-grained molecular simulation technology was employed to validate and delineate the phase transition occurring between UF molecules and amylose chains during the isothermal process. For simplicity, the model depicted in Fig. 4 includes only amylose chains (yellow particles), UF molecules (purple particles), and water molecules (blue particles). It is worth noting that the nonbonded interaction parameters corresponding to various interaction pairs are the most crucial parameters for the model. Given the stronger hydrogen bonding force between amide groups and water in UF molecules compared to that between hydroxyl groups and water in starch (Jovanović et al., 2019), coupled with the weaker cohesion among amylose at 75 °C, the interaction parameters are detailed in Table 1.

Based on Fig. 4(a) and (b), it is evident that as water evaporates, the liquid level within the model progressively decreases, and the distribution of UF and amylose shifts from initially being uniform to demonstrating gradual aggregation of UF. Additionally, the aggregation of UF resin occurs at the liquid-solid interface, the inside of the gel, and also at the gas-liquid interface. Fig. 4(c) and (d) are the snapshot photographs corresponding to Fig. 4(a) and (b), providing a clearer illustration of the distribution. The distribution of UF in Fig. 4(b) confirms the previous discussion for G70/UF gel as shown in Fig. 3(c). The video of the model can be viewed in Video Clip S3.

3.5. Application of G70/UF gel for plywood preparation

Using G70/UF gel for the production of three-layer plywood, the images are presented in Fig. 5(a). The plywood, with a thickness of 12 mm, underwent a 3-point bending test to assess its flexural properties, indicative of interfacial strength (adherence) (Birro et al., 2021), as depicted in Fig. 5(b) and Fig. 5(c). In plywood, flexural properties not only gauge the hardness of the original wooden boards but also reflect adhesive bonding characteristics. Weak bonding may result in layer slippage and deformation, adversely affecting plywood's load-bearing capacity (Stoeckel et al., 2013).

Specifically, in the dry state, plywood bonded with PVAc gel exhibited the highest flexural strength and the lowest flexural strain, while those bonded with NCS/UF gels demonstrated the lowest strength and the highest strain. In the wet state (after soaking in water for 2 h), G70/UF gel-bonded plywood exhibited the highest strength and lowest strain. Besides, the flexural properties of plywood with UF resin were assessed, but the material was too rigid to bend and exceeded the measurement range of the textural analyzer (TPA).

Consequently, UF resin demonstrated superior adhesive ability and water resistance. Compared with PVAc, G70/UF gel-bonded plywood displayed lower strength in the dry state but exhibited superior water resistance, whereas NCS/UF gel-bonded plywood showed the least adherence.

Examining the fire retardancy of plywood, in Fig. 5(d) and Video Clip S1, G70/UF gel was applied to the surface of a wooden board. When the board was exposed to the flame from a spray gun, the coated gel promptly transformed into coke. Coke, with its high carbon content, retarded fire by demanding higher oxygen concentration for combustion support (Camino et al., 1991). In Fig. 1(c) and Video Clip S2, the plywood, bonded together by G70/UF gel, was subjected to the flame from the spray gun, and the flame was rapidly extinguished upon removal of the gun. These observations highlight the crucial role played by the adhesive in enhancing the overall flame-retardant properties.

As illustrated in Fig. 5(e), the LOI for plywood bonded with PVAc and UF resin falls between 21 and 27, classifying them as combustible materials. In contrast, plywood bonded with G70/UF gel achieved an LOI of around 70, categorizing it as a non-flammable material (Donmez Cavdar, 2014). The flame retardancy can be contributed by the high concentration of Ca^{2+} in the gel. During burning, Ca^{2+} readily reacts with oxygen to produce oxides, thereby consuming oxygen, hindering the complete combustion of the gel and wooden boards, and promoting the formation of coke (Liu et al., 2023).

In summary, Fig. 5 demonstrates that employing G70/UF gel for plywood production significantly reduces the amount of UF resin while providing plywood with commendable bending resistance in both dry and wet states, along with excellent flame retardancy.

4. Conclusion

In this paper, the UF resin was introduced into the starch-based gels (10:1, starch versus UF resin, *w*/w) to improve their adhesive ability for plywood. The results demonstrate that with high amylose content (68 %) suitable isothermal parameters (75 °C and 4 h) and $CaCl_2$ concentration (33 % $CaCl_2$ solution), the shear stress of G70/UF gel significantly increased to 4.13 ± 0.12 MPa, which was higher than that of PVAc. Moreover, in a wet state (2 h of water soaking), the shear stress of G70/UF gel was 0.93 ± 0.07 MPa, and this had no significant variations during 15-day storage. Besides, because of the high Ca^{2+} ratio, the G70/UF gel exhibited flame-retardancy, and the plywood bonded by it could act as a fire deterrent, preventing the spread of flames. In contrast, with the low amylose content (27 %), the addition of UF resin had no improvement on NCS/UF gel.

Then, why did amylose content caused such significant differences between G70/UF gel and NCS/UF gel in properties? We propose this should be ascribed to amylose tending to entangle with each other, which facilitates the phase separation of UF molecules. Moreover, with water migration during the isothermal process, UF molecules cure at the interface, enhancing the adhesive property of G70/UF gel. In contrast, amylopectin, which has hydroxyl groups in high density and strong hydration ability, can hinder the phase separation and migration of UF molecules and their enrichment on the interface, leading to minimal improvement with the addition of UF resin in NCS gel (the amylopectin matrix).

In all, based on the high amylose content and isothermal process, the G70/UF gel presents a promising alternative for plywood production, reducing the usage of unhealthy UF resin while offering satisfactory bonding resistance in diverse conditions and superior flame retardancy.

Supplementary data to this article can be found online at https://doi.org/10.1016/j.carbpol.2024.122247.

CRediT authorship contribution statement

Yaoxing Chen: Validation, Methodology, Investigation, Formal analysis, Data curation. **Yongjing Rao:** Validation, Methodology, Investigation, Formal analysis, Data curation. **Peng Liu:** Writing – original draft, Visualization, Supervision, Resources, Project administration, Methodology, Funding acquisition, Conceptualization. **Linlin Wu:** Investigation, Data curation. **Guojie Zhang:** Resources, Methodology. **Jianguo Zhang:** Data curation, Formal analysis, Investigation, Methodology, Visualization. **Fengwei Xie:** Writing – review & editing, Resources, Methodology, Conceptualization.

Declaration of competing interest

The authors declare the following financial interests/personal relationships which may be considered as potential competing interests: Peng Liu reports financial support was provided by Special Fund for Scientific and Technological Innovation in Guangdong Province. Peng Liu reports financial support was provided by College Student Innovation Training Program by Guangzhou University. Peng Liu reports financial support was provided by China Scholarship Council. Fengwei Xie reports financial support was provided by Engineering and Physical Sciences Research Council. If there are other authors, they declare that they have no known competing financial interests or personal relationships that could have appeared to influence the work reported in this paper.

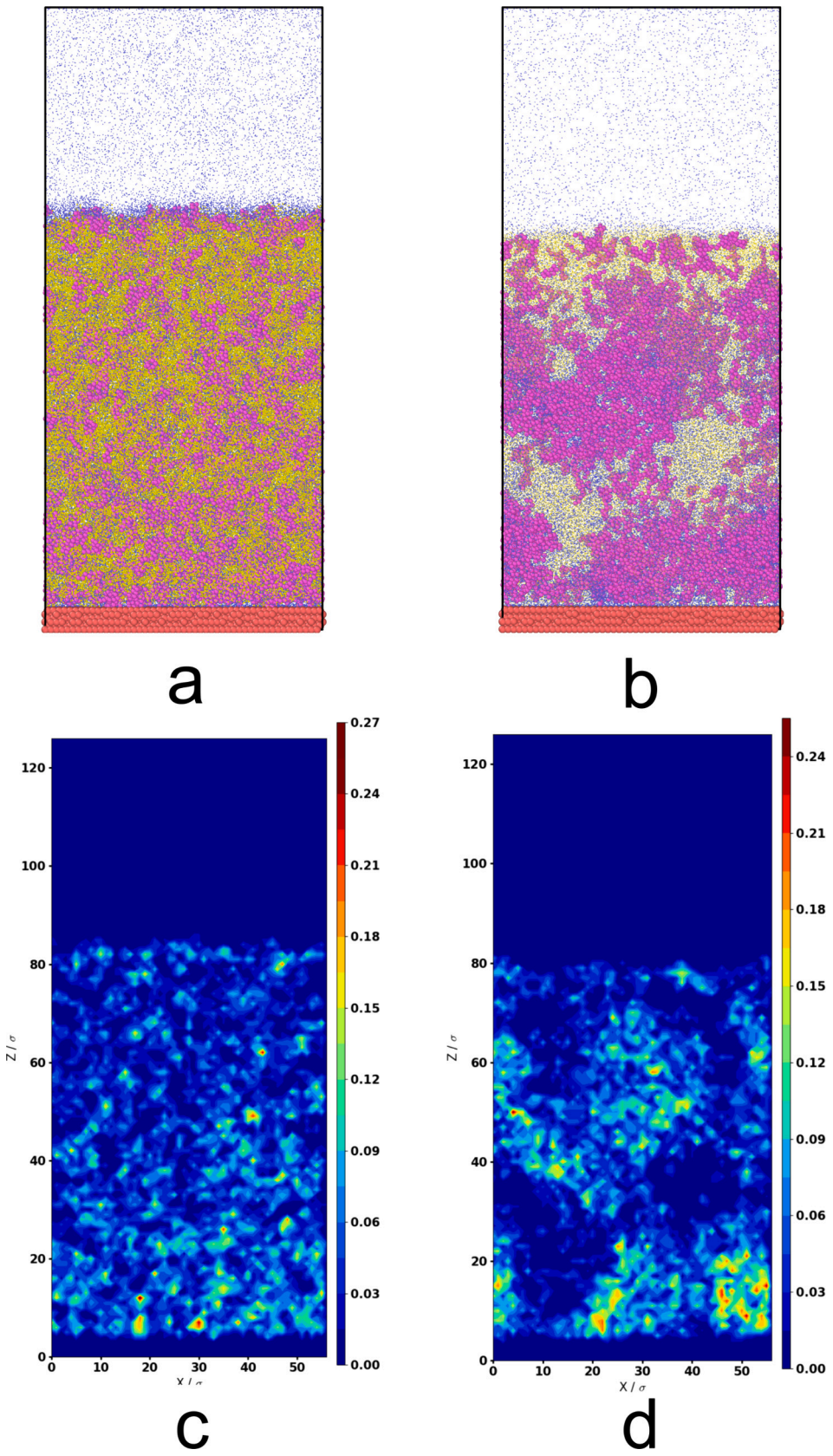

Fig. 4. Snap photos of the simulation box. (a) and (b) are the initial and final states of the simulation. Among different colored particles, yellow ones are amylose chains, purple ones are UF molecules, blue ones are water molecules, and red ones are the wooden board. (c) and (d) are the particle density plots for UF molecules, corresponding to (a) and (b), respectively.

a

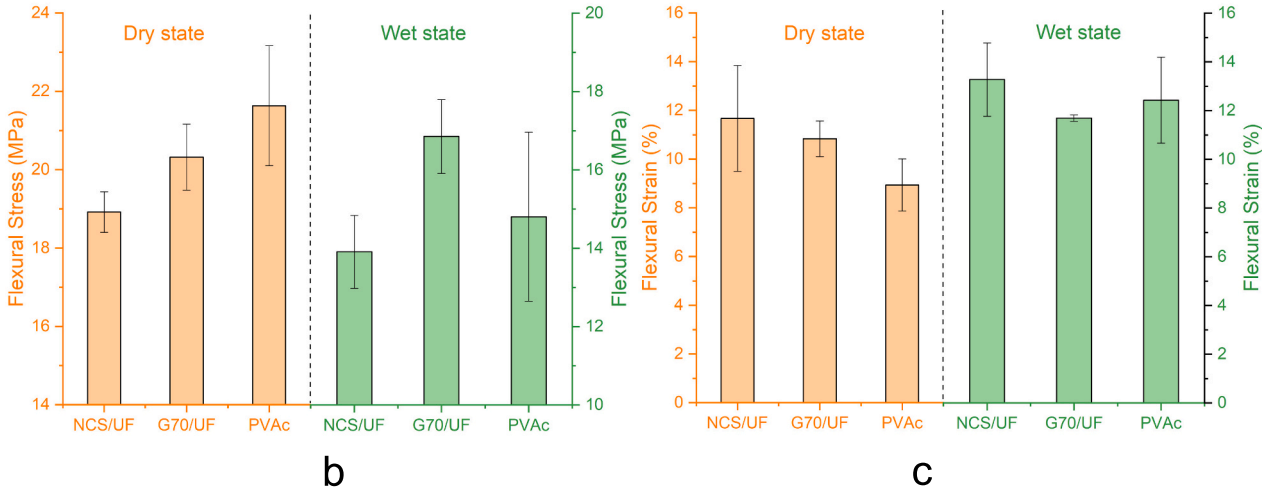

b c

d

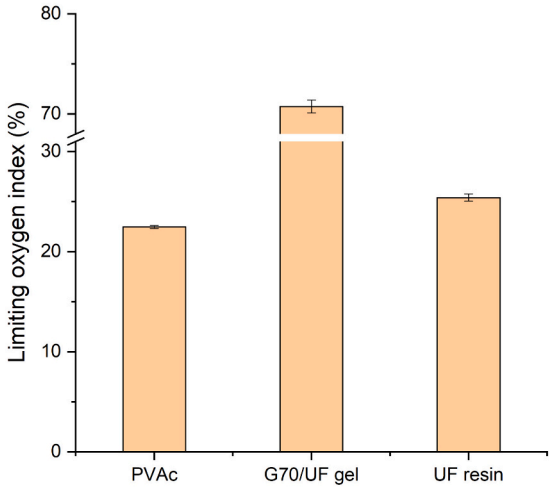

e

Fig. 5. Application of G70/UF gel to prepare plywood. (a) Photograph of plywood; (b) and (c) Flexural strength and flexural strain of the plywood for 3-point bending; (d) Photograph showing the fire retardancy of the gel when being coated on the board surface; (e) Limiting oxygen index (LOI) values of plywood bonded by different gels.

Data availability

Data will be made available on request.

Acknowledgement

This research was funded by the Special Fund for Scientific and Technological Innovation in Guangdong Province (the "Climbing Program" Special Fund) (grant no. pdjh2023b0413), the College Student Innovation Training Program by Guangzhou University (S202311078042). Peng Liu also acknowledges the China Scholarship Council (CSC) for this visiting research at Newcastle University, UK. F. Xie acknowledges funding from the Engineering and Physical Sciences Research Council (EPSRC) [grant number EP/V002236/3].

References

Arp, C. G., Correa, M. J., & Ferrero, C. (2020). Kinetic study of staling in breads with high-amylose resistant starch. *Food Hydrocolloids, 106*, Article 105879.

Baba, H., Yoshioka, R., Takatori, S., Oe, Y., & Yoshikawa, K. (2021). Transitions among cracking, peeling and homogenization on drying of an aqueous solution containing glucose and starch. *Chemistry Letters, 50*(5), 1011–1014.

BeMiller, J. N. (2011). Pasting, paste, and gel properties of starch–hydrocolloid combinations. *Carbohydrate Polymers, 86*(2), 386–423.

Birro, T. V., Aufray, M., Paroissien, E., & Lachaud, F. (2021). Assessment of interface failure behaviour for brittle adhesive using the three-point bending test. *International Journal of Adhesion and Adhesives, 110*, Article 102891.

Camino, G., Costa, L., & Luda di Cortemiglia, M. P. (1991). Overview of fire retardant mechanisms. *Polymer Degradation and Stability, 33*(2), 131–154.

Chen, L., Wang, Y., Zia ud, D., Fei, P., Jin, W., Xiong, H., & Wang, Z. (2017). Enhancing the performance of starch-based wood adhesive by silane coupling agent(KH570). *International Journal of Biological Macromolecules, 104*, 137–144.

Chiang, T. C., Hamdan, S., & Osman, M. S. (2016). Urea formaldehyde composites reinforced with sago fibres analysis by FTIR, TGA, and DSC. *Advances in Materials Science and Engineering, 2016*, 5954636.

Din, Z.-U., Chen, L., Xiong, H., Wang, Z., Ullah, I., Lei, W., … Khan, S. A. (2020). Starch: An undisputed potential candidate and sustainable resource for the development of wood adhesive. *Starch - Stärke, 72*(3–4), 1900276.

Diyana, Z. N., Jumaidin, R., Selamat, M. Z., Ghazali, I., Julmohammad, N., Huda, N., & Ilyas, R. A. (2021). Physical properties of thermoplastic starch derived from natural resources and its blends: A review. *Polymers, 13*(9), 1396.

Donmez Cavdar, A. (2014). Effect of various wood preservatives on limiting oxygen index levels of fir wood. *Measurement, 50*, 279–284.

Dorieh, A., Selakjani, P. P., Shahavi, M. H., Pizzi, A., Ghafari Movahed, S., Farajollah Pour, M., & Aghaei, R. (2022). Recent developments in the performance of micro/nanoparticle-modified urea-formaldehyde resins used as wood-based composite binders: A review. *International Journal of Adhesion and Adhesives, 114*, Article 103106.

Dunky, M. (2003). In A. Pizzi, & K. L. Mittal (Eds.), *47 Adhesives in the wood industry. Handbook of Adhesive Technology, Revised and Expanded* (2nd Ed, pp. 887–956). Taylor & Francis.

Fu, Z., Chen, J., Luo, S. J., Liu, C. M., & Liu, W. (2014). Effect of food additives on starch retrogradation: A review. *Starch - Stärke, 67*(1–2), 69–78.

Gadhave, R., V., Mahanwar, P. A., & Gadekar, P. T. (2017). Starch-based adhesives for wood/wood composite bonding: Review. *Open Journal of Polymer Chemistry, 07*(02), 19–32.

Jarusombuti, S., Bauchongkol, P., Hiziroglu, S., & Fueangvivat, V. (2012). Properties of rubberwood medium-density fiberboard bonded with starch and urea-formaldehyde. *Forest Products Journal, 62*(1), 58–62.

Jovanović, V., Samaržija-Jovanović, S., Petković, B., Milićević, Z., Marković, G., & Marinović-Cincović, M. (2019). Biocomposites based on cellulose and starch modified urea-formaldehyde resin: Hydrolytic, thermal, and radiation stability. *Polymer Composites, 40*(4), 1287–1294.

Kizil, R., Irudayaraj, J., & Seetharaman, K. (2002). Characterization of irradiated starches by using FT-Raman and FTIR spectroscopy. *Journal of Agricultural and Food Chemistry, 50*(14), 3912–3918.

Koshevoy, E. I., Samsonenko, D. G., Berezin, A. S., & Fedin, V. P. (2019). Metal-organic coordination polymers formed from γ-cyclodextrinand divalent metal ions. *European Journal of Inorganic Chemistry, 2019*, 4321–4327.

Kremer, K., & Grest, G. S. (1990). Dynamics of entangled linear polymer melts: A molecular-dynamics simulation. *The Journal of Chemical Physics, 92*, 5057–5086.

Li, H., Gidley, M. J., & Dhital, S. (2019). High-amylose starches to bridge the "Fiber gap": Development, structure, and nutritional functionality. *Comprehensive Reviews in Food Science and Food Safety, 18*(2), 362–379.

Li, J.-Z., Li, W.-J., Zhou, W.-R., Fan, D.-B., & Gao, W. (2007). Curing mechanism of urea-formaldehyde resin and its application. *Journal of Beijing Forestry University, 29*(4), 90–94.

Li, Y., Liu, P., Ma, C., Zhang, N., Shang, X., Wang, L., & Xie, F. (2020). Structural disorganization and chain aggregation of high-amylose starch in different chloride salt solutions. *ACS Sustainable Chemistry & Engineering, 8*(12), 4838–4847.

Liu, P., Ling, J., Mao, T., Liu, F., Zhou, W., Zhang, G., & Xie, F. (2023). Adhesive and flame-retardant properties of starch/Ca(2+) gels with different amylose contents. *Molecules, 28*(11), 4543.

Liu, P., Ma, C., Li, Y., Wang, L., Wei, L., Yan, Y., & Xie, F. (2020). Facile preparation of eco-friendly, flexible starch-based materials with ionic conductivity and strain-responsiveness. *ACS Sustainable Chemistry & Engineering, 8*, 19117–19128.

Long, Y., & Christie, G. (2005). Microstructure and mechanical properties of orientated thermoplastic starches. *Journal of Materials Science|Journal of Materials Science, 40*(1), 111–116.

Mandala, I., Michon, C., & Launay, B. (2004). Phase and rheological behaviors of xanthan/amylose and xanthan/starch mixed systems. *Carbohydrate Polymers, 58*(3), 285–292.

Maulana, M. I., Lubis, M. A. R., Febrianto, F., Hua, L. S., Iswanto, A. H., Antov, P., … Todaro, L. (2022). Environmentally friendly starch-based adhesives for bonding high-performance wood composites: A review. *Forests, 13*(10), 1614.

Obadi, M., Qi, Y., & Xu, B. (2023). High-amylose maize starch: Structure, properties, modifications and industrial applications. *Carbohydrate Polymers, 299*, Article 120185.

Oktay, S., Kızılcan, N., & Bengu, B. (2021). Oxidized cornstarch – Urea wood adhesive for interior particleboard production. *International Journal of Adhesion and Adhesives, 110*, Article 102947.

Oktay, S., Kızılcan, N., & Bengü, B. (2022). Environment-friendly cornstarch and tannin-based wood adhesives for interior particleboard production as an alternative to formaldehyde-based wood adhesives. *Pigment & Resin Technology, 53*(2), 173–182.

Onusseit, H. (1992). Starch in industrial adhesives: New developments. *Industrial Crops and Products, 1*(2), 141–146.

Piculell, L., Bergfeldt, K., & Nilsson, S. (1995). Factors determining phase behaviour of multi component polymer systems. In S. E. Harding, S. E. Hill, & J. R. Mitchell (Eds.), *Biopolymer Mixtures* (pp. 13–35). Nottingham: Nottingham University Press.

Plimpton, S. J. (1995). Fast parallel algorithms for short-range molecular dynamics. *J. Comp. Phys., 117*, 1–19.

Qi, Z., & Can, W. (2013). Starch evidence of glutinous plant content as the additive to Ming Great Wall mortar at Gubeikou, Beijing. *Quaternary Sciences, 33*(3), 575–581.

Radley, J. A. (1976). Adhesives from Starch and Dextrin. In A. Radley (Ed.), *Industrial uses of starch and its derivatives* (pp. 1–50). Springer.

Stoeckel, F., Konnerth, J., & Gindl-Altmutter, W. (2013). Mechanical properties of adhesives for bonding wood—A review. *International Journal of Adhesion and Adhesives, 45*, 32–41.

Sulaiman, N. S., Hashim, R., Sulaiman, O., Nasir, M., Amini, M. H. M., & Hiziroglu, S. (2018). Partial replacement of urea-formaldehyde with modified oil palm starch based adhesive to fabricate particleboard. *International Journal of Adhesion and Adhesives, 84*, 1–8.

Tester, R. F., & Sommerville, M. D. (2003). The effects of non-starch polysaccharides on the extent of gelatinisation, swelling and α-amylase hydrolysis of maize and wheat starches. *Food Hydrocolloids, 17*(1), 41–54.

Vineeth, S. K., & Gadhave, R. V. (2024). Corn starch blended polyvinyl alcohol adhesive chemically modified by crosslinking and its applicability as polyvinyl acetate wood adhesive. *Polymer Bulletin, 81*, 811–825.

Wang, H., Liang, J., Zhang, J., Zhou, X., & Du, G. (2017). Performance of urea-formaldehyde adhesive with oxidized cassava starch. *Bioresources, 12*(4), 7590–7600.

Watcharakitti, J., Win, E. E., Nimnuan, J., & Smith, S. M. (2022). Modified starch-based adhesives: A review. *Polymers, 14*(10), 2023.

Xi, W., Liu, P., Ling, J., Xian, D., Wu, L., Yuan, Y., … Xie, F. (2024). Pre-gelatinized high-amylose starch enables easy preparation of flexible and antimicrobial composite films for fresh fruit preservation. *International Journal of Biological Macromolecules, 254*, Article 127938.

Zia ud, D., Chen, L., Ullah, I., Wang, P. K., Javaid, A. B., Hu, C., … Wang, Z. (2018). Synthesis and characterization of starch-g-poly(vinyl acetate-*co*-butyl acrylate) bio-based adhesive for wood application. *International Journal of Biological Macromolecules, 114*, 1186–1193.

Zia-ud-Din, Xiong, H., & Fei, P. (2017). Physical and chemical modification of starches: A review. *Critical Reviews in Food Science and Nutrition, 57*(12), 2691–2705.